Scientific Article

Low-cost optical scanner and 3-dimensional printing technology to create lead shielding for radiation therapy of facial skin cancer: First clinical case series

Ankur Sharma MD [a,b], David Sasaki MSc [b,c], Daniel W. Rickey PhD [b,c,d], Ahmet Leylek MD [a,b], Chad Harris [c], Kate Johnson MD [a,b], Jorge E. Alpuche Aviles PhD [b,c,d], Boyd McCurdy PhD [b,c,d], Andy Egtberts [c], Rashmi Koul MBBS [a,b], Arbind Dubey MBBS [a,b],*

[a] *Department of Radiation Oncology, CancerCare Manitoba, Winnipeg, Manitoba, Canada*
[b] *Department of Radiology, University of Manitoba, Winnipeg, Manitoba, Canada*
[c] *Department of Medical Physics, CancerCare Manitoba, Winnipeg, Manitoba, Canada*
[d] *Department of Physics and Astronomy, University of Manitoba, Winnipeg, Manitoba, Canada*

Abstract

Purpose: Three-dimensional printing has been implemented at our institution to create customized treatment accessories, including lead shields used during radiation therapy for facial skin cancer. To effectively use 3-dimensional printing, the topography of the patient must first be acquired. We evaluated a low-cost, structured-light, 3-dimensional, optical scanner to assess the clinical viability of this technology.

Methods and materials: For ease of use, the scanner was mounted to a simple gantry that guided its motion and maintained an optimum distance between the scanner and the object. To characterize the spatial accuracy of the scanner, we used a geometric phantom and an anthropomorphic head phantom. The geometric phantom was machined from plastic and included hemispherical and tetrahedral protrusions that were roughly the dimensions of an average forehead and nose, respectively. Polygon meshes acquired by the optical scanner were compared with meshes generated from high-resolution computed tomography images. Most optical scans contained minor artifacts. Using an algorithm that calculated the distances between the 2 meshes, we found that most of the optical scanner measurements agreed with those from the computed tomography scanner within approximately 1 mm for the geometric phantom and approximately 2 mm for the head phantom. We used this optical scanner along with 3-dimensional printer technology to create custom lead shields for 10 patients receiving orthovoltage treatments of nonmelanoma skin cancers of the face. Patient, tumor, and treatment data were documented.

Results: Lead shields created using this approach were accurate, fitting the contours of each patient's face. This process added to patient convenience and addressed potential claustrophobia and medical inability to lie supine.

Conclusions: The scanner was found to be clinically acceptable, and we suggest that the use of an optical scanner and 3-dimensional printer technology become the new standard of care to generate lead shielding for orthovoltage radiation therapy of nonmelanoma facial skin cancer.

Introduction

The first uses of 3-dimensional printing in medicine appeared shortly after its invention.[1] Three-dimensional printing is now well established in clinical practices that range from surgical planning[2,3] to individualized medical implants.[4] For radiation therapy applications, cancer treatment centers, including ours, are currently implementing 3-dimensional printing to create customized accessories including shielding, boluses, and immobilization.[5] To create accurate accessories, the topography of the patient must be known and is typically acquired using computed tomography (CT).[6,7] Although CT has excellent geometric fidelity, it is resource intensive and excessive because it exposes the patient to unnecessary radiation, especially when only topography is required.

Optical scanning offers an alternative approach for acquiring 3-dimensional images, and a number of technologies have been developed.[8,9] Even though optical scanning has been used for radiation therapy applications,[10] these scanners are relatively expensive. Recently, 3-dimensional optical scanners have been developed for the consumer market that are low cost and can quickly acquire both topographical and textural information of a patient. Because of their low cost, a radiation therapy department can evaluate this technology without having to justify an expensive purchase.

Three-dimensional printing is a complimentary technology to optical scanning. The use of 3-dimensional printing technology is well suited for the treatment of superficially located tumors, specifically nonmelanoma skin cancer, which is the most common form of cancer.[11] This technology has been shown to improve the dosimetric conformity of skin bolus by improving the fit of the bolus on complex skin surfaces and thus reducing air gaps.[5,12] Consequently, the clinical use of 3-dimensional printed bolus is emerging as an alternative to commercially made bolus.[13,14] This technology can also be used for the creation of lead shielding,[10] which is needed to protect vulnerable organs at risk when using orthovoltage energy radiation.

Orthovoltage radiation therapy is commonly used during treatment of nonmelanoma facial skin cancers as a widely accepted alternative to surgical resection.[15] However, the creation of the shielding can be especially difficult because of the many complex contours of the human face. Conventional methodology involves creating a plaster of Paris model of the patient's face by first creating a negative impression mold of the face while the patients is lying supine. This mold is then filled with plaster of Paris to create a positive model of the face. Subsequently, a thin layer of lead is formed to the surface of the positive model.

A limitation of this approach is the need for a number of patient visits. Because of mobility and transportation issues, these visits are especially difficult for elderly patients, in whom radiation therapy is more commonly used. Because patients are required to have plaster laid over their face, this approach is also not appropriate for patients who are claustrophobic or medically unable to lie supine for long periods of time. A solution to these problems is to use optical scanning to quickly acquire an image of the patient's face and then use a 3-dimensional printer to produce the required model.

In this paper, we characterize a structured, light, 3-dimensional optical scanner and use a scanning gantry to assess the clinical viability of this technology for radiation therapy. We also show how the optical scanner can be used with 3-dimensional printer technology to create lead shields for use in orthovoltage radiation therapy of nonmelanoma skin cancers of the face. We report the first institutional experience of using these shields to treat 10 patients.

Methods and materials

The optical scanner (Fig 1A) is a consumer-grade device (3D Systems Sense) that uses a structured infrared light source along with an infrared camera to determine the location of points on an object's surface. Most of the data processing is handled by proprietary hardware (PrimeSense Carmine) within the scanner, as described elsewhere.[16,17] The scanner also has a visible-light camera that acquires photographic (texture) data. The use of this particular type of consumer-grade optical scanner is limited within radiation oncology; however, Park et al have successfully used a similar device to create compensators used in total body irradiation.[18]

The optical scanner is designed to be handheld or mounted on a tripod. We found that this scanner required all data to be acquired in 1 pass (ie, the patient had to remain within the field of view, or tracking was lost). In addition,
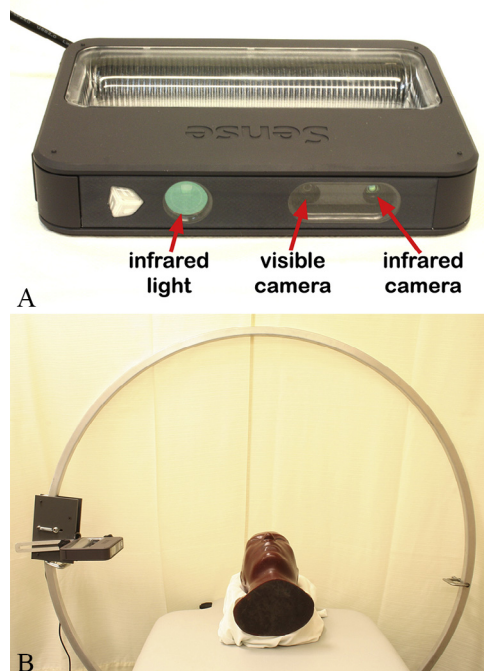
Figure 1 (A) Optical scanner used to acquire 3-dimensional images. Structured light is projected in the infrared and detected with a camera. (B) Gantry and optical scanner. The scanner is moved by hand. The bed height can be adjusted to place the scan region at the isocenter.

Figure 2 (A) Renderings of meshes from (left) computed tomography and (right) optical scans of the geometric phantom. A number of artifacts are visible in the optical scan. (B) The effect of the field-of-view setting on the root mean square differences between meshes obtained with computed tomography and the optical scanner. Results are for the geometric phantom and show that reducing the field of view generally increases the accuracy of the optical measurements.

the manufacturer indicated that the minimum scanner-to-patient distance was 35 cm. Moving the scanner too close or too far from the patient resulted in data truncation (ie, no measurements). Thus, for ease of use, the scanner was mounted to a simple gantry (Fig 1B) that guided its motion. This gantry was manufactured in-house and consisted of a circular hoop formed from square aluminum tubing with a diameter of 126.5 cm.

The optical scanner was mounted to an arm that could be moved isocentrically along the circumference of the hoop. The scanner-to-surface distance was adjustable to accommodate differently sized regions of the body. The gantry could also tilt through ±20 degrees with respect to the patient table, allowing for acquisition of topography from various directions. The distance from the isocenter to the table top could be adjusted by varying the table height. In this study, each scan resulted in a 3-dimensional triangulated mesh that was saved to disc in polygon file format, which described a single object consisting of polygons.

Scanner characterization

To characterize the spatial accuracy of the scanner, 2 phantoms were used. The first was a geometric phantom (Fig 2A) that we designed using CAD software (SolidEdge, Siemens) and machined from plastic with a
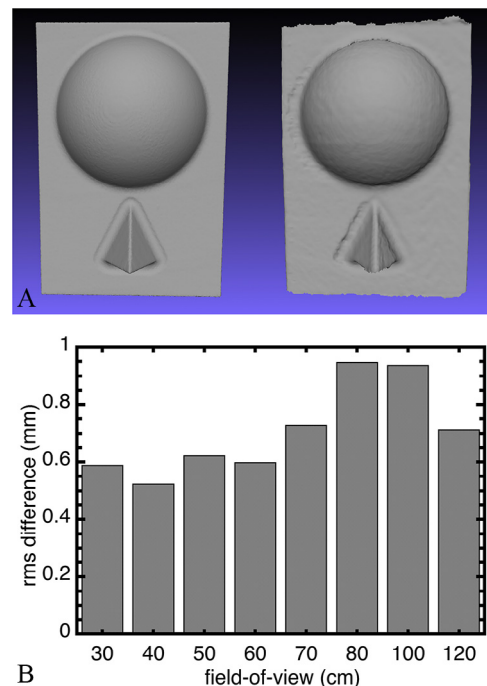
computer-controlled milling machine (Haas Automation). This phantom had overall dimensions of 24×15 cm and included a hemispherical and a tetrahedral protrusion of roughly the dimensions of an average forehead and nose, respectively.[19]

The second phantom was an anthropomorphic head (Fig 3A), which was originally intended for radiographic imaging (manufacturer unknown). To obtain images with the optical scanner, each phantom was placed at the isocenter of the gantry, and the optical scanner was moved by hand in an arc about the isocenter. Scans also included tilting the gantry through a range of approximately ±15 degrees while the scanner was at the 12 o'clock position. The head phantom was positioned so that the field of view was centered about the nose. The optical scanner's acquisition software was set to give the highest resolution possible.

For comparisons, both phantoms were also scanned with x-ray CT (Brilliance, Philips Medical Systems), which was taken as the gold standard for this study. CT images were acquired at a high spatial resolution (ie, 1024×1024 matrix; 0.8 mm slice thickness with 0.4 mm spacing and a field of view of 250 mm). The resulting CT images were automatically segmented with commercial software (Eclipse, Varian Medical Systems) and exported as a 3-dimensional mesh
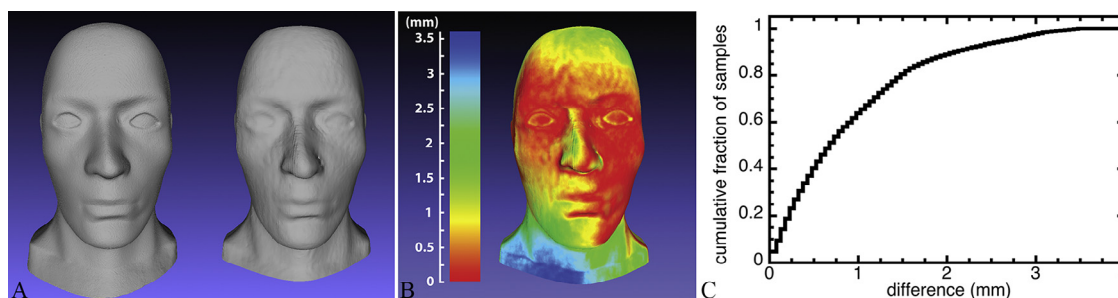
Figure 3 (A) Renderings of meshes from computed tomography (left) and optical scan (right) of a head phantom. The optical scanner produced artifacts in the region of the nose. (B) Spatial difference between the optical and computed tomography scans. (C) Cumulative frequency plot corresponding to the image shown in (B). Differences are between meshes obtained with computed tomography and the optical scanner. Most measurement points (89%) agree within 2 mm.

in stereolithography file format, which described the 3-dimensional object as a surface consisting of triangles.

To ensure that the segmentation of the CT images for each phantom was accurate, the threshold CT number was adjusted until the width of the segmented image agreed with the known width of the phantom. For optical scans of the geometric phantom, the rough edges along the bottom (where it rested on the table top) were trimmed in software (Meshmixer, Autodesk). For optical scans of the head phantom, all rough edges at the periphery of the phantom were trimmed, but no further processing was performed on the scans.

Polygon meshes acquired by the optical scanner were compared to meshes generated from the CT images using several routines that were implemented in open-source software (MeshLab).[20] To enable comparison, the 2 meshes were first aligned with each other. As a starting point, the 2 meshes were roughly aligned from several pairs of matching points that were manually selected on each mesh. Subsequently, a more refined alignment was obtained using an iterative closest point algorithm.[21] The implementation of this algorithm in Meshlab is relatively complex and relies on various optimization techniques to improve efficiency.[22]

Once aligned, we applied an algorithm, as described by Cignoni et al,[23] that calculated distances between the 2 aligned meshes. Briefly, the mesh generated by the optical scanner was sampled thousands of times. The distance between each sample's location and the nearest location in the mesh generated by the CT scanner was found. The results are shown as an image and as a cumulative frequency plot of these distances. In addition, the root mean square (RMS) distance was calculated using the same technique.

The acquisition software for the optical scanner allowed the field of view to be adjusted, which also changed the mesh density (ie, a larger field of view resulted in a lower mesh density). To evaluate the effect of the field-of-view setting, optical scans were obtained of the geometric phantom with settings that ranged from 30 cm to 120 cm.

RMS differences over this range were used to select an appropriate field-of-view setting.

Lead shielding

Between July 1, 2015 and December 1, 2016, patients with nonmelanoma skin cancers of the face who required radical radiation using low-energy photons were identified as requiring lead shielding to protect vulnerable organs at risk. Patient, tumor, and treatment-specific data were collected retrospectively using an electronic charting system (ARIA, Varian Medical Systems). These data included age at diagnosis (based on tissue biopsy), sex, tumor histology, tumor location, clinical stage, radiation dose, radiation fractionation, and treatment energy.

Patients were initially seen in the clinic by a radiation oncologist, who defined a clinical treatment field by outlining it directly on the patient with a permanent marker. This included a clinical treatment volume, planning target volume, and penumbra. Using the optical scanner, a surface image of each patient's face was obtained while the patient was lying supine. This scan usually was conducted during the patients' initial visit. Once an optical scan was obtained, mesh editing software (MeshMixer, Autodesk) was used to repair objectionable artifacts and crop the volume to a size suitable for printing. In addition, the treatment field border that was previously identified by the radiation oncologist was embossed into the mesh so that the field would be visible in the finished print. Subsequently, the files were converted to g-code, which is the numerical control programming language used to control the 3-dimensional printer, using open-source software (Slic3r).

To produce lead shields, a positive model of each face was printed on a consumer-grade 3-dimensional printer (M2, MakerGear). This printer used fused deposition modelling to lay down layers of melted thermoplastic (ie, polylactic acid). Generally, a 0.3 mm layer thickness was used. The infill settings were chosen so that the resulting models would
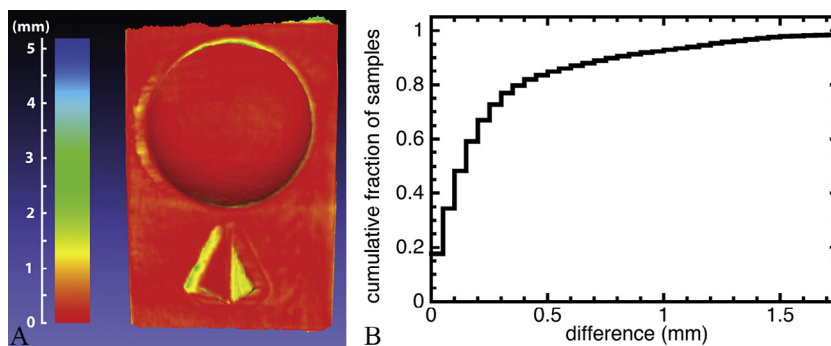
Figure 4   (A) Spatial difference between meshes obtained with the optical scanner and computed tomography (Fig 2A). The optical scanner used a 40 cm field of view. (B) Cumulative frequency plot corresponding to the image of the geometric phantom shown in (A). The differences are between the 2 meshes obtained with computed tomography and the optical scanner. Most measurement points (93%) agree within 1 mm.

be very rigid and durable. To improve print quality, the printer was operated at a relatively slow speed of 30 mm/second. The print time was approximately 12 hours per model.

The resulting model was used as a form to shape the lead. Using a hammer, a 3 mm thick layer of lead was formed to closely fit the contours of the model. An aperture was then cut into the lead shield to match the embossed field border. Finally, the lead shield was painted for protection of the patient and staff. Each lead shield was placed on the patient's face during radiation treatment delivery to protect the organs at risk.

Ethics approval and institutional review board reference numbers were obtained through the University Health Research Ethics Board and our facility's Research Resource Impact Committee.

Results

Scanner characterization

The total time to acquire an optical scan using the gantry was approximately 1 minute. A typical optical scan of the geometric phantom is shown in Figure 2A, along with the mesh generated from the CT images for reference. The optical scan is noticeably rougher than the CT scan. Also visible are artifacts near the edges of the tetrahedron and hemisphere. These artifacts are asymmetric about the scan axis and may be a result of how the structured light source was blocked during parts of the scan.

To select an appropriate field-of-view setting, the geometric phantom was used and the RMS differences between meshes obtained with CT and with the optical scanner were calculated and plotted (Fig 2B). For all settings, the RMS difference was quite good (ie, less than 1 mm). In addition, there was a general increase in the geometric accuracy of the optical scan as the field of view was reduced. The reduction in RMS differences for field-of-view settings over

80 cm was likely due to smoothing of the data by the large mesh elements. For all subsequent measurements, the field of view was set to 40 cm because this was an appropriate size to easily acquire scans of the entire head phantom. A smaller field-of-view setting resulted in unwanted cropping, and larger settings resulted in the inclusion of extraneous details from the table and other background objects.

The spatial differences between the CT and optical data were calculated and are shown in Figure 4A as an image, where the color bar indicates the differences. Red corresponds to good agreement and blue to a difference of 5 mm. In this case, the optical data were acquired with a field-of-view setting of 40 cm. Although most measurements agree well with CT, the differences are larger in regions that contain artifacts. To further quantify these measurements, a cumulative frequency plot of the differences is shown in Figure 4B. It can be seen that most (93%) of the measurements made with the optical scanner agree within 1 mm of those from CT.

To simulate a more realistic case, the previous analysis was repeated with the anthropomorphic head phantom, and the resulting optical and CT scans are shown in Figure 3A. There are artifacts on and close to the nose. The spatial differences between the CT and optical data were calculated and are shown in Figure 3B. The largest difference is in the shoulder region, which was well away from the center of the optical scan. These results are quantified as a cumulative frequency plot (Fig 3C), in which most (89%) of the measurements made with the optical scanner agree within 2 mm of those from CT.

Lead shielding

Ten patients were identified as requiring lead shielding. Details of the patients' tumor and treatment data are listed in Table 1. Seven patients were female, and 3 were male. The average age at diagnosis was 75.5 years. Two

Table 1   Patient, tumor, and treatment characteristics

Patient number	Sex	Age (y)	Histology	Location	Stage	Dose (Gy)	Fractions	Energy (kV)
1	M	76	BCC	Nose	T1N0	40	10	250
2	F	78	BCC	Nose	T2N0	40	10	250
3	M	77	BCC	Nose	T1N0	40	10	250
4	F	84	1) BCC	1) Nose	1) T1N0	1) 40	1) 10	1) 250
			2) BCC	2) Nose	2) T1N0	2) 40	2) 10	2) 250
5	F	69	BCC	Nose	T1N0	40	10	250
6	F	78	BCC	Nose	T1N0	36	6	100
7	M	67	BCC	Nose	T2N0	30	5	180
8	F	85	PNT/MCC	Nose	T1N0	55	22	250
9	F	79	BCC	Nose	T1N0	40	10	250
10	F	62	1) BCC	1) Nose	1) T1N0	1) 55	1) 22	1) 250
			2) BCC	2) Lip	2) T1N0	2) 55	2) 22	2) 250

BCC, basal cell carcinoma; F, female; M, male; PNT/MCC, primary neuroendocrine tumor/Merkel cell carcinoma.

patients had concurrent diagnoses of 2 skin cancers (patients 4 and 10), for a total of 12 tumors in the study. Eleven of 12 tumors were determined to be basal cell carcinoma by biopsy. All but 1 tumor was located on the nose. Ten of 12 tumors were staged as T1N0, and 10 of 12 tumors were treated with radical-intent radiation therapy. One patient with Merkel cell carcinoma was treated with palliative-intent radiation therapy. Only 1 patient (patient 1) had radical surgical resection and went on to receive adjuvant intent radiation therapy. Most tumors (7 of 12) were treated with a radiation dose of 40 Gy in 10 fractions. Ten of the 12 tumors were treated with a beam energy of 250 kV.

Once the clinical treatment field was defined by the oncologist, the optical scan was acquired quickly (in approximately 1 minute) and without incident in all 10 cases. An example using a volunteer is shown in Figure 5. We found that the resulting optical scans allowed for offline treatment planning without further inconvenience to the patient. Interdisciplinary discussions were held prior to the manufacture of the lead shield to define various parameters, including the extent of the lead shield needed to adequately cover the organs at risk. The printing of the facial models took approximately 12 hours each. No significant

issues were reported by the physicians, physicists, or radiation therapists when using this technique.

All lead shields were successfully used during radiation treatment in all 10 patients. For each of the 10 patients, the fit of the shield and the accuracy of the treatment field border was assessed by the radiation oncologist. In all 10 cases, the fit was deemed acceptable, and the patients did not report any physical discomfort or feelings of claustrophobia. Acceptable protection of organs at risk was confirmed by visual inspection in all cases. At our institution, this approach has become the standard of care for creating lead shielding for the treatment of nonmelanoma skin cancers of the face.

Discussion

An optical scanner and gantry have been evaluated and found to enable quick and easy acquisition of topographical information. Although the optical scanner can be used freehand, we found that using the gantry made acquisition much easier by maintaining an optimum distance between the scanner and the object. The gantry diameter
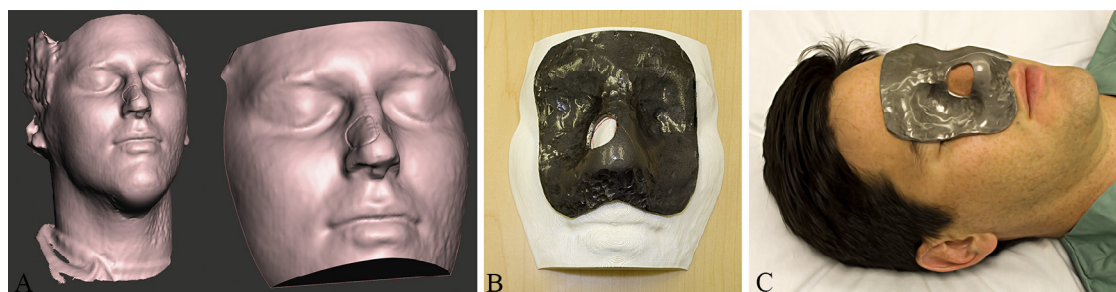

Figure 5   (A) On the left is the unaltered data obtained with the optical scanner. On the right is the final, edited data set that was used to print the 3-dimensional model. (B) The 3-dimensional printed model with a 3 mm lead shield molded to fit the complex facial contours. Also visible is the cutout area representing the clinical treatment field on the right side of the nose. (C) The final product, the lead shield sits on the volunteer patient's face, offering protection of the organs at risk from radiation damage.

was constrained by the minimum scanner-to-patient distance, the intended use, and the overall height. This gantry was intended primarily for scanning the head and may need to be larger if body scans of large patients are required. However, too large a gantry could be impractical for some staff because it may be too high to easily operate.

We found that tilting the gantry at the 12 o'clock position allowed for better coverage of the nostrils. However, this technique was limited because the gantry pivoted about its bottom, which caused the head to move out of the field of view when the tilt angle exceeded 15 degrees. Future designs would be improved by having the tilt take place about the isocenter. The gantry also ensured that scans were performed in a consistent and reproducible manner, which is important when the resulting images are used in the treatment of patients. Because the time to acquire a scan was approximately 1 minute, motion artifacts are not expected to be a major concern. The gantry was built in-house with a total cost of approximately $500; it is very lightweight and easy to setup and store.

Most of the scans contained noticeable artifacts (Figs 2A and 4A) although in most instances these were considered minor, either because they were small (less than 1 mm) or easily removable with postprocessing techniques. In general, artifacts presented as either surface roughness or localized indentations. We found that objectionable artifacts could be rendered insignificant by straight-forward postprocessing in software such as MeshMixer because most artifacts were small and easily distinguished from the true contours and consequently could be replaced by a smoothed surface. During clinical use, optical scans were inspected immediately after acquisition to ensure that the quality was adequate for the intended task. Because the acquisition time was approximately 1 minute, a scan was repeated very quickly when needed. Although postprocessing was always required before the mesh could be used to design treatment accessories, it was often a quick task (eg, 10 minutes).

We found that the scanner's 40 cm field-of-view setting was an appropriate size for head scans and provided good accuracy (Fig 2B). As described, a limitation of the optical scanner is that all data had to be acquired in 1 pass (ie, patient or table always had to be in the field of view, or tracking was lost). For larger scans (eg, of the legs), the gantry could be modified by allowing the table to travel. Otherwise, separate scans could be acquired and then combined in software such as Meshlab. The visible-light camera incorporated into the scanner was sufficient for acquiring skin markings, typically used to delineate treatment regions, which is important for planning treatments and designing accessories. Because its light source is invisible, the optical scanner is well suited for scanning anxious patients who would otherwise be stressed by alternate scanning techniques.

In a radiation therapy facility, patient contours are typically acquired using either CT or a medium such as plaster of Paris, depending on the application. When comparing the acquisition of contours using the optical scanner with those using traditional molding techniques (eg, plaster of Paris), there are 2 distinct advantages: 1) there is no requirement for direct patient contact, which can cause discomfort when there is disease on the surface of the skin, and 2) the time that the patient's presence is required is greatly reduced because the scan time is short compared with the time required to create a traditional mold. Both of these should help improve the patient experience.

Scanning is also advantageous in patients who are claustrophobic and cannot tolerate a plaster mask. By using optical scanner technology, this source of potential patient anxiety is completely removed. In addition, optical scanner technology is immensely helpful when treating patients who cannot lie supine for prolonged periods because of conditions such as congestive heart failure or lung disease. These conditions are more commonly seen in elderly patients, who are more likely to be treated with radical radiation therapy as opposed to surgical resection. Using optical scanner and 3-dimensional printer technology also adds to patient convenience. The optical scan can be performed on the same day as the initial patient appointment, which eliminates additional clinical visits that are necessary when using conventional methods. This is especially important in elderly populations who are more likely to have mobility issues or less likely to drive or otherwise get to medical appointments.

One goal of this paper was to compare the performance of the optical scanner with the very best tool available clinically (ie, CT). If the optical scanner generates images with resolution similar to that of the CT scanner, the optical scanner should be acceptable for clinical use. A comparison of the optical and high-resolution CT scans shows that the 2 techniques agreed within approximately 2 mm (Figs 3 and 4). However, Ogden et al showed that the choice of CT acquisition parameters and segmentation method will affect the resulting accuracy.[24] We minimized these systematic errors by choosing thresholds so that the segmentations agreed with the known dimensions of the phantoms. The field of view used for Figure 3 was much larger than required to produce a lead shield; the agreement between CT and the optical scanner would have been improved if the images were cropped. However, these results would be useful in the case of producing a large bolus or large immobilization device.

The resolution of the optical scanner is clinically acceptable for a number of radiation therapy applications. As described, we routinely use this optical scanner along with a 3-dimensional printer to design lead shielding for low-energy photon treatments. We also intend to use the optical scanner to design other customized treatment accessories, including immobilization and bolus for photon and electron treatments.

One potential concern is that inaccuracies in a scan used to design an accessory could result in small air gaps between the accessory and the patient surface. This could have implications for the fit of the accessory, the reproducibility of accessory placement, and the dosimetry if the accessory

is used as a bolus material. However, for electron treatments, a small air gap between the skin and bolus has no significant effect.[25,26] For photon treatments, air gaps of less than a few millimeters are anticipated to have no significant effect on the surface dose.[27-29] In practice, the actual effect of an air gap is nuanced and depends on the details of a treatment, and one should consider this effect for each specific case. For routine clinical work, we recommend that a quality assurance program be implemented; this could be as simple as regularly scanning and printing objects with known dimensions.

We have described how to use this technology to make lead shielding for 10 patients. For each of the 10 patients in this study, a qualitative inspection by the oncologist verified that the shielding had an excellent fit and provided excellent protection to the organs at risk. In principle, a more quantitative assessment of the fit would have been desirable; however, the lead shielding precluded imaging with CT or magnetic resonance imaging. The reliance on a qualitative assessment is acceptable because any air gaps between the shielding and skin would not have compromised protection of the organs at risk. Consequently, it was not critical to have an exact fit.

Although we included only a small number of study patients within a single institutional setting, we found that this approach had a number of advantages over the traditional molding technique that uses plaster of Paris. The main advantages were the noncontact method of manufacture and the ability to quickly scan the patient. Secondary benefits included a reduction in manual labor and in mess such as dust. Because the optical scanner was quite compact, it required a modest amount of clinic space.

If a lead shield needs to be remade because of damage or necessary modifications, this is easy to do by using either the existing face model or by reprinting another model based on the original scan. This saves physician time, and there is no need for the patient to return for an extra appointment. This could eventually lead to substantial cost savings because it may be possible for more patients to be seen in a timely manner. Our experience is consistent with that of Canters et al,[13] who demonstrated that 3-dimensional printing technology in the radiation oncology setting can save substantial amounts of valuable time for both radiation therapists and physicians.

For this work, the choice of printer is important. These models use a relatively large amount of consumables, and cost must be considered when choosing a printer. We used a consumer-grade 3-dimensional printer, not only because of its low capital cost but more importantly because of the low cost of consumables (eg, polylactic acid filament). Although the models may take approximately 12 hours to print, the 3-dimensional printer runs overnight and unsupervised. Of note, we deliberately slowed the print time to improve quality and reduce the probability of a print failure.

A significant advantage of using these lead plates is their low cost. The process of hammering the lead and cutting

the aperture was fairly quick (eg, approximately 15 minutes). There are alternative 3-dimensional printing methods for producing the shields, such as pouring molten lead or Cerrobend into a 3-dimensional printed mold.[30] Stereolithography is excellent for producing high-quality molds and can easily accommodate hot Cerrobend. A mold for a face mask would be printed as 2 or 3 pieces. All 3-dimensional printing approaches require some degree of postprocessing, and these mold pieces would require removal of supports and cleaning. After removal of mold flash and painting, the final product would be a very good-looking shield, although functionally equivalent to the shield described in this manuscript.

Printing the shield with a 3-dimensional printer that directly prints metals[31] is an interesting consideration. Unfortunately, printers that are capable of printing metal are currently intended for high-value applications such as aerospace and surgical implants and may be too expensive for this application.[32] We do not know of any printers that work with pure lead, but an interesting option would be to use fused deposition modeling with a filament containing tungsten (eg, GMass, Turner Medtech). Because this filament has a density that is approximately half that of lead, the shield would need to be approximately twice as thick. Regardless of the manufacturing process, the shield and its aperture would always be verified by an oncologist.

The use of optical scanner and 3-dimensional printer technology requires a high level of technical knowledge, which was provided by the medical physics department at our institution. Those implementing this technology at other centers may struggle with its steep learning curve. This problem can be remedied by using an interdisciplinary approach, as we did at our center. We found that with increased clinical usage, there was a commensurate increase in institutional confidence and comfort level.

Conclusions

The geometric accuracy of the optical scanner is acceptable for radiation therapy purposes. We found the scanner to be clinically acceptable and have used it along with 3-dimensional printer technology to create lead shielding used in the treatment of skin cancers of the face. This method worked extremely well, and we will continue to increase its use at our center. We recommend that easily implementable optical scanner and 3-dimensional printer technology be adopted as the new standard of care for creating lead shielding used in the orthovoltage radiotherapeutic management of nonmelanoma skin cancers of the face.

References

1. Palser R, Jamieson R, Sutherland JB, Skibo L. Three-dimensional lithographic model building from volume data sets. *Can Assoc Radiol J*. 1990;41:339-341.

2. Choi J, Kim N. Clinical application of three-dimensional printing technology in craniofacial plastic surgery. *Arch Plast Surg*. 2015;42:267-277.

3. Succo G, Berrone M, Battiston B, et al. Step-by-step surgical technique for mandibular reconstruction with fibular free flap: Application of digital technology in virtual surgical planning. *Eur Arch Otorhinolaryngol*. 2015;272:1491-1501.

4. Shan XF, Chen HM, Liang J, Huang JW, Cai ZG. Surgical reconstruction of maxillary and mandibular defects using a printed titanium mesh. *J Oral Maxillofac Surg*. 2015;73:1437, e1-9.

5. Kim SW, Shin HJ, Kay CS, Son SH. A customized bolus produced using a 3-dimensional printer for radiotherapy. *PLoS ONE*. 2014;9:e110746.

6. Evans PM. Anatomical imaging for radiotherapy. *Phys Med Biol*. 2008;53:R151-R191.

7. Burleson S, Baker J, Hsia AT, Xu Z. Use of 3D printers to create a patient-specific 3D bolus for external beam therapy. *J Appl Clin Med Phys*. 2015;16:5247.

8. Sansoni G, Trebeschi M, Docchio F. State-of-the-art and applications of 3D imaging sensors in industry, cultural heritage, medicine, and criminal investigation. *Sensors (Basel)*. 2009;9:568-601.

9. Shin B, Venkatramani R, Borker P, Olch A, Grimm J, Wong K. Spatial accuracy of a low cost high resolution 3D surface imaging device for medical applications. *Int J Med Phys Clin Eng Radiat Oncol*. 2013;2:45-51.

10. Zemnick C, Woodhouse SA, Gewanter RM, Raphael M, Piro JD. Rapid prototyping technique for creating a radiation shield. *J Prosthet Dent*. 2007;97:236-241.

11. Rogers HW, Weinstock MA, Harris AR, et al. Incidence estimate of nonmelanoma skin cancer in the United States, 2006. *Arch Dermatol*. 2010;146:283-287.

12. Su S, Moran K, Robar JL. Design and production of 3D printed bolus for electron radiation therapy. *J Appl Clin Med Phys*. 2014;15:4831.

13. Canters RA, Lips IM, Wendling M, et al. Clinical implementation of 3D printing in the construction of patient specific bolus for electron beam radiotherapy for non-melanoma skin cancer. *Radiother Oncol*. 2016;121:148-153.

14. Park JW, Yea JW. Three-dimensional customized bolus for intensity-modulated radiotherapy in a patient with Kimura's disease involving the auricle. *Cancer Radiother*. 2016;20:205-209.

15. Rong Y, Zuo L, Shang L, Bazan JG. Radiotherapy treatment for nonmelanoma skin cancer. *Expert Rev Anticancer Ther*. 2015;15:765-776.

16. Diaz MG, Tombari F, Rodriguez-Gonzalvez P, Gonzalez-Aguilera D. Analysis and evaluation between the first and the second generation of RGB-D sensors. *IEEE Sens J*. 2015;15:6507-6516.

17. Difilippo NM, Jouaneh MK. Characterization of different Microsoft Kinect sensor models. *IEEE Sens J*. 2015;15:4554-4564.

18. Park SY, Kim J, Joo YH, Lee JC, Park JM. Total body irradiation with a compensator fabricated using a 3D optical scanner and a 3D printer. *Phys Med Biol*. 2017;62:3735-3756.

19. Department of Defense, Human Factors Engineering Technical Advisory Group. *Human Engineering Design Data Digest*. Washington, DC: 2000.

20. Cignoni P, Callieri M, Corsini M, Dellepiane M, Ganovelli F, Ranzuglia G. MeshLab: An open-source mesh processing tool. *Eurographics Ital Chapter Conf*. 2008;129-136.

21. Besl PJ, McKay ND. A method for registration of 3-D shapes. *IEEE Trans Pattern Anal Mach Intell*. 1992;14:239-253.

22. Rusinkiewicz S, Levoy M. Efficient variants of the ICP algorithm. *3-D Digit Imaging Model*. 2001;145-152.

23. Cignoni P, Rocchini C, Scopigno R. Metro: Measuring error on simplified surfaces. *Comput Graph Forum*. 1998;17:167-174.

24. Ogden KM, Aslan C, Ordway N, Diallo D, Tillapaugh-Fay G, Soman P. Factors affecting dimensional accuracy of 3-D printed anatomical structures derived from CT data. *J Digit Imaging*. 2015;28:654-663.

25. Kong M, Holloway L. An investigation of central axis depth dose distribution perturbation due to an air gap between patient and bolus for electron beams. *Australas Phys Eng Sci Med*. 2007;30:111-119.

26. Sharma SC, Johnson MW. Surface dose perturbation due to air gap between patient and bolus for electron beams. *Med Phys*. 1993;20:377-378.

27. Butson MJ, Cheung T, Yu P, Metcalfe P. Effects on skin dose from unwanted air gaps under bolus in photon beam radiotherapy. *Radiat Meas*. 2000;32:201-204.

28. Chung JB, Kim JS, Kim IA, Lee JW. Surface dose measurements from air gaps under a bolus by using a MOSFET dosimeter in clinical oblique photon beams. *J Korean Phys Soc*. 2012;61:1143-1147.

29. Khan Y, Villarreal-Barajas JE, Udowicz M, et al. Clinical and dosimetric implications of air gaps between bolus and skin surface during radiation therapy. *J Cancer Ther*. 2013;4:1251-1255.

30. Zhu X, Driewer J, Li S, et al. Fabricating Cerrobend grids with 3D printing for spatially modulated radiation therapy: A feasibility study. *Med Phys*. 2015;42:6269-6273.

31. Wang L, Cao T, Li X, Huang L. Three-dimensional printing titanium ribs for complex reconstruction after extensive posterolateral chest wall resection in lung cancer. *J Thorac Cardiovasc Surg*. 2016;152:e5-e7.

32. Thomas DS, Gilbert SW. Costs and cost effectiveness of additive manufacturing: A literature review and discussion. *NIST Spec Publ 1176*. 2014. doi:10.6028/NIST.SP.1176.